Controlling chaos by negative feedback of subharmonic components

R. Meucci, A. Labate, and M. Ciofini
Istituto Nazionale di Ottica, Largo E. Fermi 6, 50125 Florence, Italy
(Received 8 May 1997)

In this paper we present a control technique for stabilizing chaotic motion to periodic orbits in a CO_2 laser with electro-optic feedback. The control method is based on negative feedback of subharmonic components of the laser intensity signal. A detailed analysis, performed using the four-level model for the CO_2 laser, allows us both to reproduce the experimental features and to compare our method with the time-delayed autosynchronization method introduced by Pyragas [Phys. Lett. A **170**, 421 (1992)]. [S1063-651X(97)13809-0]

PACS number(s): 05.45.+b, 42.50.Lc, 42.55.Lt

INTRODUCTION

The possibility of directing chaotic dynamics to periodic orbits or steady states by applying small amplitude perturbations has opened new perspectives in the theory and applications of nonlinear dynamics. The interest in this field was increased after the development of ''tracking'' and ''targeting'' algorithms. Tracking algorithms, based on the control method proposed by Ott, Grebogi, and Yorke (OGY) [1] and on other control systems [2], allow us to follow unstable fixed points or unstable periodic orbits embedded in different dynamical regimes as the control parameter is changed [3–7]. Targeting procedures deal with the problem to rapidly direct the motion, originated from a given initial condition on a chaotic attractor, to a small target region by using a sequence of small, time dependent changes to one or more suitable parameters [8,9].

The aim of the present work is to provide experimental evidence of stabilization of periodic orbits embedded in the chaotic attractor of an autonomous system, namely a CO_2 laser with electro-optic regenerative feedback [10]. In this configuration, the degree of freedom necessary to observe the transition to chaos is obtained by feeding the laser output back to an intracavity electro-optic modulator. An additional negative feedback, obtained after a selective filtering of the subharmonic components present in the chaotic laser intensity, is used to direct the system towards stable orbits. This frequency domain approach to control of chaos, at variance with other methods that require a knowledge of the phase-space topology (as the OGY), appears particularly suitable for systems characterized by fast dynamics, and presents strong analogies with the time-delayed autosynchronization (TDAS) method introduced by Pyragas [11]. The method has been applied by Bielawski *et al.* to a CO_2 laser with modulated losses [12], and several variations have been proposed [13,14].

The results of our experiment can be reproduced in terms of the so-called four-level model for the CO_2 laser, which has been demonstrated to adequately fit the chaotic dynamics of the CO_2 laser with electro-optic feedback [15].

EXPERIMENTAL RESULTS

The experimental configuration employed in this work is reported in Fig. 1 and it concerns a single mode CO_2 laser with an intracavity loss modulator driven by a voltage V. The intensity decay rate k of the cavity depends on V as

$$k(V)=k_0\left[1+k_1\sin^2\left(\frac{\pi(V-V_0)}{V_\lambda}\right)\right], \tag{1}$$

where $k_0=cT/L$ ($L=1.35$ m is the cavity length and $T=0.09$ is the total transmission coefficient for a single pass), $k_1=(1-2T)/2T$, $V_\lambda=4240$ V is the half-wave voltage of the modulator, and $V_0=100$ V an offset accounting for a small misalignment between the optical axis of the modulator crystal and the intracavity polarization direction imposed by the Brewster windows. The voltage V is obtained through a feedback loop which includes an HgCdTe detector revealing the laser intensity, a preamplifier, and an high-voltage differential amplifier. A bias voltage B, representing the control parameter, is finally added to V, which obeys the following equation:

$$\dot{V}=-\beta\left(V-B+\frac{RI}{1+\alpha I}\right), \tag{2}$$

where $\beta=300$ kHz is the damping rate of the feedback loop, I is the adimensional laser intensity, and $R=6.6\times10^{-10}$ is the total gain of the feedback loop. The term αI ($\alpha=1.2\times10^{-13}$) takes into account the nonlinearity of the detection apparatus.

Once the pump and the gain of the feedback loop are selected, B acts as the control parameter of the system. Upon increasing B, the system passes from a stable point (constant

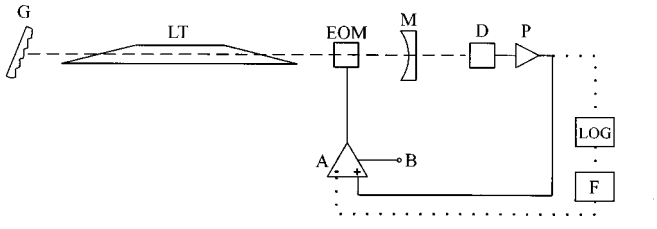

FIG. 1. Experimental setup. G, diffraction grating; LT, laser tube; EOM, electro-optic modulator; M, outcoupling mirror; D, HgCdTe detector; P, preamplifier; A, differential amplifier; B, bias input; LOG, logarithmic converter; F, washout filter. The dotted line represents the control feedback loop.

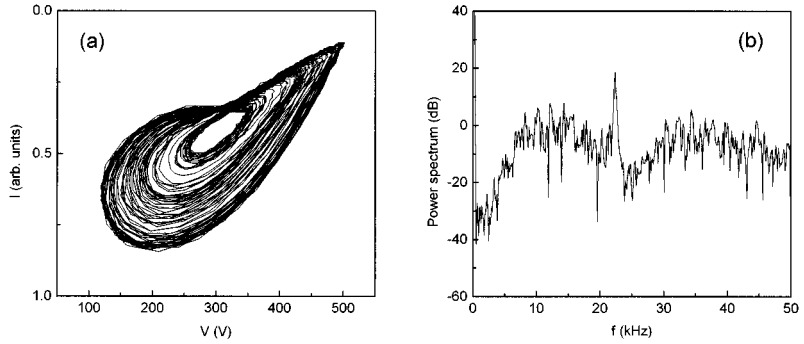

FIG. 2. Experimental results. (a) Phase space plot (laser intensity I vs feedback voltage V) for the unperturbed chaotic attractor. (b) Power spectrum corresponding to (a).

laser output) to a limit cycle through a Hopf bifurcation and then the chaotic behavior is reached after a sequence of subharmonic bifurcations. The chaotic attractor ($B=360$ V), reported in Fig. 2(a), is obtained by plotting the laser intensity I versus the voltage V. The corresponding broadband power spectrum is presented in Fig. 2(b) and it clearly shows the presence of a peak at a frequency $f\approx 22$ kHz, which is close to that of the limit cycle originated at the Hopf bifurcation. This feature is crucial for the choice of the control used to select and stabilize periodic orbits contained in the chaotic attractor. Apart from the phase-space plot of the attractor and its power spectrum, the chaotic nature is also proved by the evaluation of the correlation dimension of the intensity temporal signal, estimated with the Grassberger and Procaccia algorithm [16] to be $D_2=2.10\pm 0.04$.

The spectral analysis of the chaotic signal suggests the possibility of adopting a control method based on a negative feedback loop where all the unwanted frequency components are transmitted by a selective filter (F in Fig. 1) as correction signals. The only frequency components not affected by the control loop are the zero frequency (which controls the long time behavior) and the frequency still evident above the broad continuum in the chaotic spectrum, corresponding to the cycle to be stabilized. These results have been achieved by means of a selective filter, known also as ''washout filter'' [17], whose transfer function (Fig. 3) matches the above requirements. The filter input is driven by a signal proportional to the laser intensity (Fig. 1), while the output is fed back to the negative input of the high voltage differential amplifier. In Fig. 4(a) we report the stabilized orbit of period 1 when the feedback control loop has been activated. In order to characterize the control performance, we estimate the relative perturbation introduced as the ratio between the filter output and the amplified laser intensity (i.e., the ratio between the two input signals of the high-voltage amplifier); since this ratio is roughly 7% we are confident that the stabilized orbit is only slightly different from that embedded in the chaotic attractor. Note that the filter has been implemented with the possibility of tuning the notch point in a range of $\pm 10\%$ around 23 kHz. However, we have not found relevant changes in the control loop performance within the above range.

Finally, if the controller is modified inserting a logarithmic amplifier (LOG in Fig. 1) to drive the filter, its performances increase, providing stabilization of period-1 orbit [Fig. 4(b)] with smaller values of the relative perturbation (about 4.5%). The reasons to employ the logarithmic amplifier will be clarified in the next section, which is devoted to the analysis of the theoretical model.

The presented measurements allow us to compare this feedback control method to an alternative strategy which uses a nonfeedback method, based on the application of a small sinusoidal perturbation to the bias voltage B, at frequencies close to the leading frequency of the broadband chaotic spectrum [18]. In such a case, stabilization of period-2 and period-4 orbits has been obtained by choosing perturbations with relative amplitudes of the same order as those applied in the case of the feedback method. However, it is important to note that with this nonfeedback method the frequencies of the stabilized orbits are locked to the external perturbation frequency, in agreement with the theory of periodic perturbation of autonomous systems [19]. Furthermore, stabilization of the period-1 orbit implies a remarkable deformation of the orbit itself, which can be no longer identified as that embedded in the chaotic attractor.

THE MODEL

The model is based on the standard four-level scheme for the CO_2 laser, which consists of five differential equations involving the laser intensity I, the populations of the lasing levels N_1 and N_2, and the global populations of the rotational manifolds M_1 and M_2 [15]. Consequently, the dynamics of our system, including the electro-optic feedback, is ruled by the following set of differential equations:

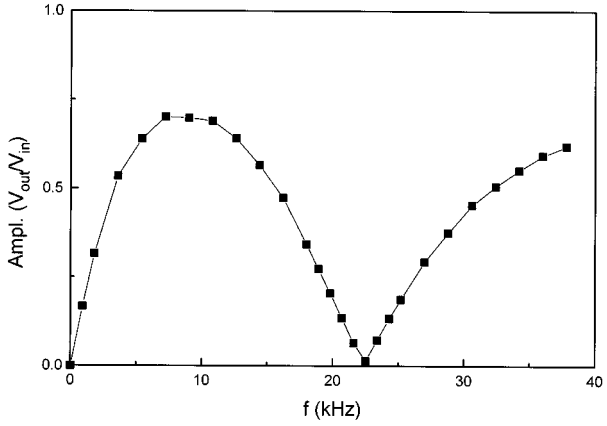

FIG. 3. Amplitude response of the filter as a function of the frequency f.

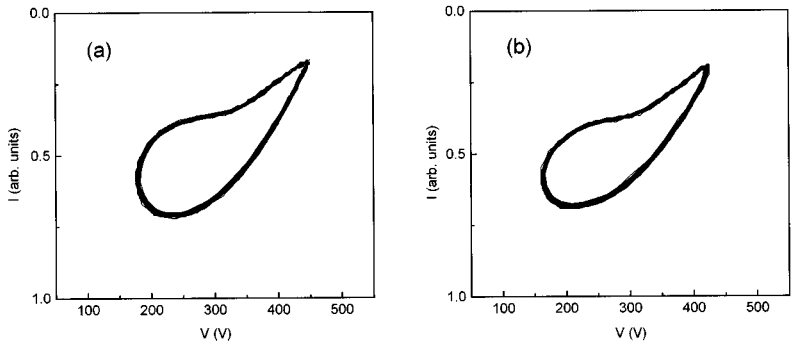

FIG. 4. (a) Stabilized orbit (I vs V) of period 1 obtained when the feedback control loop consists of only the selective filter $C(s)$ (linear control). (b) Stabilized orbit of period 1 when the logarithmic amplifier is added to the feedback control loop (nonlinear control).

$$
\begin{aligned}
\dot{I} &= I[-k(V)+G(N_2-N_1)],\\
\dot{N}_1 &= -(z\gamma_R+\gamma_1)N_1+G(N_2-N_1)I+\gamma_R M_1,\\
\dot{N}_2 &= -(z\gamma_R+\gamma_2)N_2-G(N_2-N_1)I+\gamma_R M_2+\gamma_2 P,\\
\dot{M}_1 &= -(\gamma_R+\gamma_1)M_1+z\gamma_R N_1,\\
\dot{M}_2 &= -(\gamma_R+\gamma_2)M_2+z\gamma_R N_2+z\gamma_2 P,\\
\dot{V} &= -\beta\left(V-B+\frac{RI}{1+\alpha I}\right),
\end{aligned}
\tag{3}
$$

where $G=7.3\times10^{-8}\text{sec}^{-1}$ is the field-matter coupling constant, $\gamma_R=7.0\times10^5\ \text{sec}^{-1}$ is the relaxation rate between the lasing states and the associated rotational manifolds (the enhancement factor $z=10$ represents the number of sublevels considered in each manifold), $\gamma_1=8.0\times10^4\ \text{sec}^{-1}$ and $\gamma_2=1.0\times10^4\ \text{sec}^{-1}$ are the relaxation rates of the vibrational states, and the adimensional parameter $P=3.06\times10^{14}$ represents the pump. The numerical values of these quantities are deduced from Ref. [15], except the value of the pump parameter P and the gain R, which have been changed due to the different experimental conditions. In particular, we observe that the frequency of the leading cycle of the chaotic attractor is around 22 kHz (instead of 38 kHz), as a consequence of operating at a lower value of the discharge current and at higher gain.

It is useful to introduce the following order ≈ 1 variables:

$$
\begin{aligned}
x_1 &= \frac{G}{k_0}I, \qquad (4)\\
x_2 &= \frac{G}{k_0}(N_2-N_1),\\
x_3 &= \frac{G}{k_0}(N_2+N_1),\\
x_4 &= \frac{G}{k_0}(M_2-M_1),\\
x_5 &= \frac{G}{k_0}(M_2+M_1),\\
x_6 &= \frac{\pi}{V_\lambda}(V-V_0),\\
\tau &= t\gamma_R .
\end{aligned}
$$

If we set

$$
f(x_1)=\frac{\tilde{R}x_1}{1+\tilde{\alpha}x_1},
$$

where $\tilde{R}=(\pi k_0/GV_\lambda)R$ and $\tilde{\alpha}=(k_0/G)\alpha$, Eqs. (3) can be rewritten as

$$
\begin{aligned}
\dot{x}_1 &= \tilde{k}_0 x_1[x_2-1-\tilde{k}_1\sin^2(x_6)],\\
\dot{x}_2 &= -\Gamma_1 x_2-2\tilde{k}_0 x_2 x_1+\gamma x_3+x_4+P_0,\\
\dot{x}_3 &= -\Gamma_1 x_3-x_5+\gamma x_2+P_0,\\
\dot{x}_4 &= -\Gamma_2 x_4-\gamma x_5+z x_2+z P_0,\\
\dot{x}_5 &= -\Gamma_2 x_5-z x_3+\gamma x_4+z P_0,\\
\dot{x}_6 &= -\tilde{\beta}x_6+\tilde{\beta}B_0-\tilde{\beta}f(x_1),
\end{aligned}
\tag{5}
$$

where we set

$$
\begin{aligned}
B_0 &= \frac{\pi}{V_\lambda}(B-V_0),\\
\tilde{k}_1 &= k_1,\\
\tilde{k}_0 &= \frac{k_0}{\gamma_R},\\
\Gamma_1 &= \frac{\gamma_1+\gamma_2+2z\gamma_R}{2\gamma_R},\\
\Gamma_2 &= \frac{\gamma_1+\gamma_2+2\gamma_R}{2\gamma_R},\\
\gamma &= \frac{\gamma_1-\gamma_2}{2\gamma_R},\\
P_0 &= \frac{\gamma_2 PG}{k_0\gamma_R},
\end{aligned}
$$

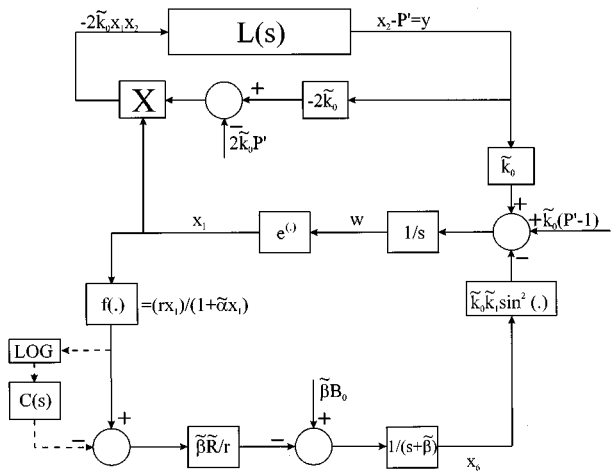

FIG. 5. Logical diagram corresponding to Eqs. (6).

$$\tilde{\beta}=\frac{\beta}{\gamma_R}.$$

By introducing the transformation $w=\log(x_1)$, Eqs. (5) can be transformed into the set

$$\begin{aligned}
\dot{w}&=\tilde{k}_0[x_2-1-\tilde{k}_1\sin^2(x_6)],\\
\dot{x}_2&=-\Gamma_1 x_2-2\tilde{k}_0 x_2 e^w+\gamma x_3+x_4+P_0,\\
\dot{x}_3&=-\Gamma_1 x_3-x_5+\gamma x_2+P_0,\\
\dot{x}_4&=-\Gamma_2 x_4-\gamma x_5+z x_2+z P_0,\\
\dot{x}_5&=-\Gamma_2 x_5-z x_3+\gamma x_4+z P_0,\\
\dot{x}_6&=-\tilde{\beta}x_6+\tilde{\beta}B_0-\tilde{\beta}f(e^w).
\end{aligned}\tag{6}$$

Considering Eqs. (6) in the frequency domain ($s=i\omega$), we can more easily separate the global dynamics in a linear and a nonlinear block as shown in Fig. 5. In this schematization, known as Lur'e representation [20], $L(s)$ represents the transfer function of the linear dynamical block. This block, corresponding to the second, third, fourth, and fifth equations of Eqs. (6), has two inputs, the constant term P_0 and the nonlinear term $-2\tilde{k}_0 x_2 e^w$, and an output x_2. The two inputs give a constant output P' and a variable output y, respectively, so that, by superposition, we have $x_2=P'+y$.

The first and the last equations of Eqs. (6) represent the feedback to the linear block. Note that the variable x_2 is not an accessible quantity in the experiment, while the variable w, neglecting the nonlinearity of the detection process, can be obtained after a logarithmic amplification of the laser intensity. In this schematization, the total gain of the feedback loop $\tilde{R}$ ($\tilde{R}=133.9$) has been splitted in two parts, r and $\tilde{R}/r$, where $r=0.1339$ is the gain associated to the optical detector (in series with the preamplifier) and $\tilde{R}/r=1000$ is the gain of the high-voltage differential amplifier.

The controller structure is reported in Fig. 5 and consists in the cascade of a nonlinear element for the logarithmic amplification and of a linear element, the selective filter, with transfer function $C(s)$. $C(s)$ fulfills the requirements given in the preceding section, i.e., it has two zeros at $\omega=0$ and $\omega=\omega_0$ (the last corresponding to the frequency still present in the chaotic spectrum) and a maximum at $\omega_0/2$. The transfer function $C(s)$ has the following analytical expression:

$$C(s)=\frac{ks(s^2+\omega_0^2)}{\left(s^2+\zeta\omega_0 s+\frac{\omega_0^2}{4}\right)(s+\mu)}.$$

Following our rescaling, the fundamental frequency $f=22.47$ kHz corresponds to $\omega_0=0.2016$; the other parameter values are $k=3.5$, $\zeta=0.7$, and $\mu=0.8$.

Figure 6(a) shows the chaotic attractor of the unperturbed system obtained from the numerical integration of Eqs. (6) for $B=223$ V, and Fig. 6(b) shows the stabilized orbit of period 1 when the controller has been activated. Thus, the model is able to reproduce the main experimental features, including the value of the relative perturbation necessary to stabilize the period-1 orbit (5%). This theoretical approach clarifies the reasons for making feedback of the variable w instead of x_1. Furthermore, numerical simulations which consider only the selective filter $C(s)$ without the nonlinearity of the logarithmic amplification, confirm stabilization of the period-1 orbit for $k=0.87$. In this case, the relative perturbation is 10%, in agreement with the experiment.

For the sake of comparison, in Fig. 6(b) we also report the stabilized orbit obtained with the TDAS control method. In this case, the controller transfer function $C(s)$ is

$$C(s)=K_c(1-e^{-sT}),$$

where $T=31.15$ is the delay time (equal to the period of the orbit to be stabilized) and $K_c=0.35$ is the gain. Although

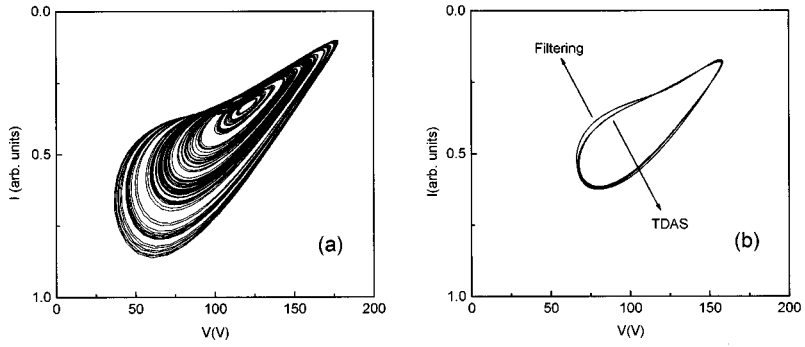

FIG. 6. Numerical results obtained by integration of Eqs. (6) for $B=223$ V. (a) Unperturbed chaotic attractor. (b) Comparison between the stabilized orbit of period 1 obtained with the selective filtering and with the TDAS method.

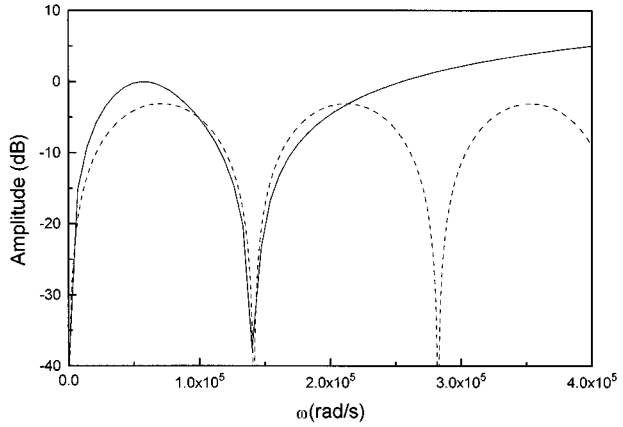

FIG. 7. Comparison between the transfer function $C(s)$ in the case of selective filtering (solid line) and in the case of TDAS (dashed line).

from a theoretical point of view the two methods are different, it is clear from Fig. 6(b) that they produce quite similar results. This suggests that the common characteristic to present a zero of the transfer function (Fig. 7) at the frequency ω_0 is sufficient to obtain a satisfactory stabilization. From Fig. 7 we can note that, at variance with our case, the TDAS transfer function amplitude goes to zero also for all ω_0 harmonics. This ensures that the stabilized limit cycle is exactly the one of the unperturbed chaotic attractor, and the control signal vanishes when the stabilization is obtained. Anyway, our scheme has the advantage of being more robust in real systems, because the feedback loop tends to eliminate the high frequency components [21].

Another important feature of our method concerns the position of the controller in the logical scheme (Fig. 5). If the controller is inserted in parallel with the integrator block $1/s$, its effects can be easily predicted [21,22]. Here, the only accessible point to insert the filter is along the regenerative feedback loop, between the detector and the high voltage differential amplifier. The transfer function between these two points before the insertion of the filter is $G(s)=1$.

If, for simplicity, we consider only the filter $C(s)$ (in such a case the controller is linear), the insertion of the control implies the modification of the transfer function $G(s)$ into $G'(s)=[1-C(s)]$. It can be easily verified that $G'(0)=G(0)=1$, $G'(j\omega_0)=G(j\omega_0)=1$, and $G'(j\omega)$ has a minimum for $\omega=\omega_0/2$, which means that the insertion of the filter determines cancellation of subharmonics. This local rejection of the subharmonic components is sufficient to avoid their presence throughout the system, allowing stabilization of the period-1 orbit.

CONCLUSIONS

The results of this experiment extend the validity of the feedback scheme based on the elimination of subharmonic components, when the leading frequency of the chaotic spectrum has been identified. This characteristic makes the method particularly suitable for low-dimensional chaotic systems where it is possible, from a preliminary learning session, to extract the information necessary for selective filtering in the frequency domain. Such a model-independent strategy can be easily adapted to a variety of situations, including those characterized by fast dynamics and spatiotemporal chaos [23–25].

ACKNOWLEDGMENTS

The authors wish to thank F. T. Arecchi and S. Boccaletti (Istituto Nazionale di Ottica), R. Genesio, A. Tesi, and M. Basso (Dipartimento di Sistemi e Informatica of the University of Florence) for useful discussions on the method, and F. Signorini for his relevant contribution to performing the numerical simulations. Work partly supported by the coordinated project ''Nonlinear dynamics in optical systems'' of the Italian National Council of Research.

[1] E. Ott, C. Grebogi, and J. A. Yorke, Phys. Rev. Lett. **64**, 1196 (1990); T. Shinbrot, E. Ott, C. Grebogi, and J. A. Yorke, Nature (London) **363**, 411 (1993); W. L. Ditto, S. N. Rauseo, and M. L. Spano, Phys. Rev. Lett. **65**, 3211 (1990).

[2] B. Peng, V. Petrov, and K. Showalter, J. Chem. Phys. **95**, 4957 (1991); E. R. Hunt, Phys. Rev. Lett. **67**, 1953 (1991).

[3] T. Carroll, I. Triandaf, I. B. Schwartz, and L. Pecora, Phys. Rev. A **46**, 6189 (1992); Z. Gills, C. Iwata, R. Roy, I. B. Schwartz, and I. Triandaf, Phys. Rev. Lett. **69**, 3169 (1992).

[4] V. In, W. L. Ditto, and M. L. Spano, Phys. Rev. E **51**, R2689 (1995).

[5] V. Petrov, M. J. Crowley, and K. Showalter, Phys. Rev. Lett. **72**, 2955 (1994).

[6] D. J. Christini and J. J. Collins, Phys. Rev. E **53**, R49 (1996).

[7] M. Ciofini, A. Labate, and R. Meucci, Phys. Lett. A **227**, 31 (1997).

[8] E. J. Kostelich, C. Grebogi, E. Ott, and J. A. Yorke, Phys. Rev. E **47**, 305 (1993).

[9] L. A. Komotseva, A. V. Naumenko, A. M. Samson, and S. I. Turovets, Opt. Commun. **136**, 335 (1997).

[10] F. T. Arecchi, W. Gadomski, and R. Meucci, Phys. Rev. A **34**, 1617 (1987).

[11] K. Pyragas, Phys. Lett. A **170**, 421 (1992); **206**, 323 (1995).

[12] S. Bielawski, D. Derozier, and P. Glorieux, Phys. Rev. E **49**, R971 (1994).

[13] D. J. Gauthier, D. W. Sukow, H. M. Concannon, and J. E. S. Socolar, Phys. Rev. E **50**, 2343 (1994); J. E. S. Socolar, D. W. Sukow, and D. J. Gauthier, *ibid.* **50**, 3245 (1994).

[14] S. Boccaletti and F. T. Arecchi, Europhys. Lett. **31**, 127 (1995).

[15] A. Varone, A. Politi, and M. Ciofini, Phys. Rev. A **52**, 3176 (1995).

[16] P. Grassberger and I. Procaccia, Phys. Rev. Lett. **50**, 346 (1983).

[17] R. Genesio, A. Tesi, H. O. Wang, and E. H. Abed, in *Proceedings of XXIII IEEE Conference on Decision and Control, San Antonio* (IEEE, New York, 1993).

[18] M. Ciofini, R. Meucci, and F. T. Arecchi, Phys. Rev. E **52**, 94 (1995).

[19] H. K. Khalil, *Nonlinear Systems* (MacMillan, Basingstoke, England, 1992).
[20] M. Vidyasagar, *Nonlinear System Analysis* (Prentice-Hall, Englewood Cliffs, NJ, 1993).
[21] M. Basso, R. Genesio, and A. Tesi (unpublished).
[22] R. Meucci, M. Ciofini, and R. Abbate, Phys. Rev. E **53**, R5537 (1996).
[23] W. Lu, D. Yu, and R. G. Harrison, Phys. Rev. Lett. **76**, 3316 (1996).
[24] R. Martin, A. J. Scroggie, G. L. Oppo, and W. J. Firth, Phys. Rev. Lett. **77**, 4007 (1996).
[25] S. Boccaletti, D. Maza, H. Mancini, R. Genesio, and F. T. Arecchi (private communication).